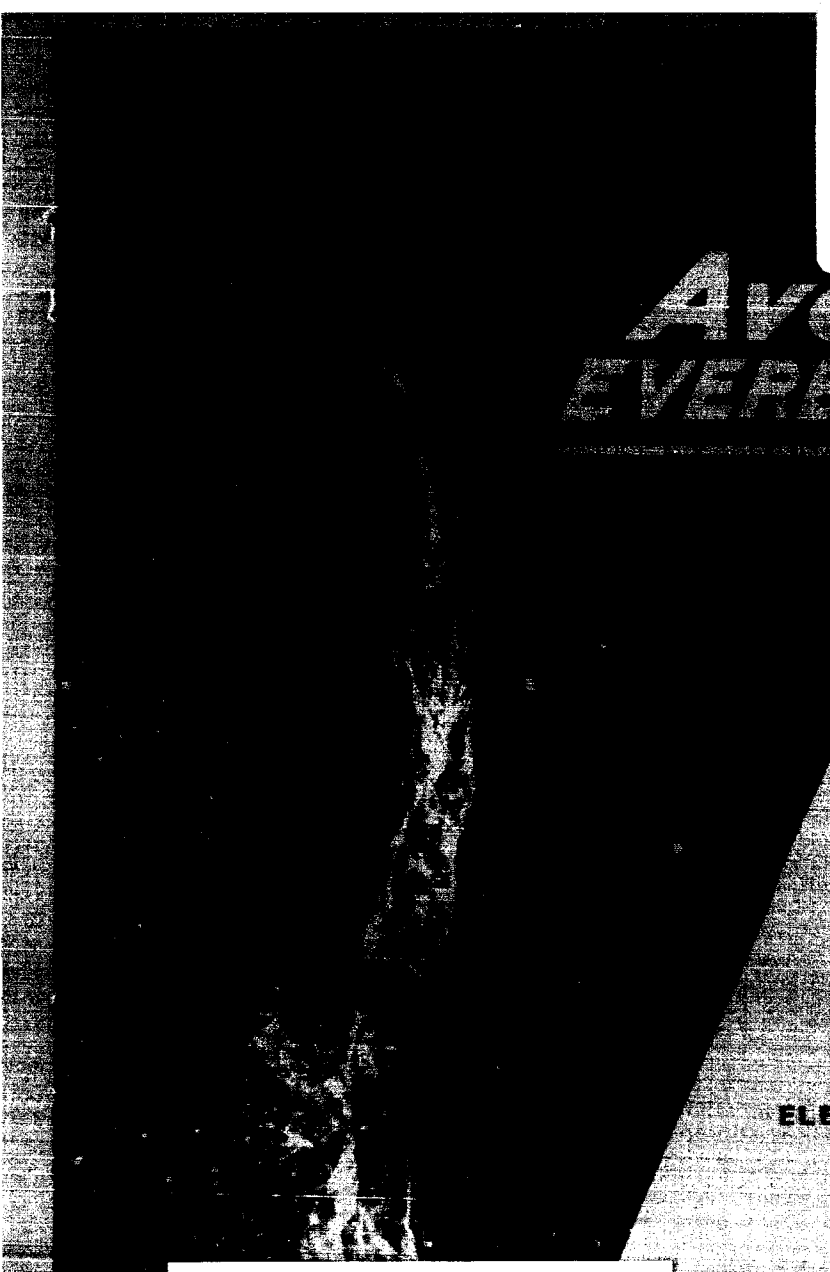

AVCO EVERETT

RESEARCH LABORATORY

a division of
AVCO CORPORATION

NONEQUILIBRIUM SHOCK FRONT ROTATIONAL, VIBRATIONAL AND ELECTRONIC TEMPERATURE MEASUREMENTS

R. A. Allen

RESEARCH REPORT 186
Contract No. NAS w-748
August 1964

prepared for
HEADQUARTERS
NATIONAL AERONAUTICS AND SPACE ADMINISTRATION
OFFICE OF ADVANCED RESEARCH AND TECHNOLOGY
Washington 25, D. C.

RESEARCH REPORT 186

NONEQUILIBRIUM SHOCK FRONT ROTATIONAL, VIBRATIONAL AND ELECTRONIC TEMPERATURE MEASUREMENTS

by

R. A. Allen

AVCO-EVERETT RESEARCH LABORATORY
a division of
AVCO CORPORATION
Everett, Massachusetts

August 1964

Contract No. NAS w-748

prepared for

HEADQUARTERS
NATIONAL AERONAUTICS AND SPACE ADMINISTRATION
OFFICE OF ADVANCED RESEARCH AND TECHNOLOGY
Washington 25, D. C.

ABSTRACT

A spectroscopic technique is described for measuring nonequilibrium shock front rotational, vibrational and electronic temperatures. This method uses a triple channel monochromator which is able to resolve the vibrational structure of diatomic molecular radiation, and a monitor channel to observe an electronic transition composed of many vibrational transitions. Measurements are made on incident nitrogen shock waves by observing the $\Delta v = +1$ sequence of the $N_2^+(1-)$ and $N_2(1+)$ systems. As well as giving nonequilibrium temperature results, this experiment has given equilibrium radiation intensities which indicate an f number at the 0, 0 transition of .035.

Author

I. INTRODUCTION

Shock front excitation and relaxation processes involving diatomic molecules determine to a large extent the flow and radiation field around hypersonic re-entry vehicles. The study of these processes is therefore quite important. For sufficiently strong shock waves, the instantaneous translational temperature just behind the shock is higher than the equilibrium temperature. The approach to equilibrium is then governed by the rates of vibrational relaxation, dissociation and ionization. During this relaxation process, electronic excitation rates can proceed sufficiently fast and are capable of producing radiation overshoots.[1] The purpose of the present work was to examine this shock front radiation in a shock tube and to develop a spectroscopic method for measuring temperatures in the relaxation zone.

The equilibrium temperature behind incident and reflected shocks has been measured by several workers using different techniques. Parkinson and Nicholls[2] used CN as a thermometric molecule to measure rotational temperatures in reflected shocks in argon. Faizullov et al[3] used sodium line reversal techniques to make time history studies of the sodium electronic temperature in incident shock waves. Wurster and Treanor,[4] employing another technique, utilized the absorption of light

by O_2. The calculated temperature dependence of the absorption allowed the temperature to be defined. More recently, Watson[5] measured temperature by observing the light emitted from OH $^2\Sigma \rightarrow {}^2\pi$ simultaneously in two separate wavelength regions. The results of these different experiments are all in general agreement with theoretically calculated equilibrium temperatures based on initial pressures and shock speeds.

One of the most interesting shock front regimes for making temperature measurements is the nonequilibrium region. Temperature measurements in this region are difficult to interpret because of the nonequilibrium nature of the gas. At any given point in the relaxation region, different temperatures can be used to describe the state of the translational, rotational, vibrational and electronic degrees of freedom. One must assume, of course, that the distribution of energy over each degree of freedom is Boltzmann-like. In a nonequilibrium gas sample, the temperature of a thermometric molecule may not be the same as that of the gas. For this reason, one of the constituent molecular radiators of the gas should be used to make meaningful nonequilibrium temperature measurements.

Qualitatively, the method used for making nonequilibrium temperature measurements on incident shocks in this study was to examine how the molecular band structure of the radiation varied in the nonequilibrium region, after normalizing to the equilibrium temperature based on the shock conditions.

II. EXPERIMENTAL

a) Shock Tube

These measurements were made in an electric arc-driven six-inch shock tube. The operation of this shock tube has been thoroughly described in the literature.[6] Measurements were made on incident nitrogen shocks viewed through copper knife edges mounted in the test section which was located 20 feet downstream from the driver. The speed was measured using photomultipliers which located the arrival of the shock wave at equally spaced locations over the last 10 feet of the tube. To keep impurities at a minimum, a flow system was used. The shock tube was pumped down to a few μ Hg pressure and allowed to outgas for several hours before each run. The resultant leak rates at the end of this period of outgassing were less than 1 μ Hg per minute.

b) Monochromator

The instrument used in these measurements was a Jarrel-Ash triple channel monochromator. The optical system was collimated by a combination of entrance slit and stop size, producing a spatial resolution of 0.5mm. The entrance slit of the monochromator was imaged on the axis of the shock tube using the usual optical train reported in the literature for making this type of measurement.[1,7] Wavelength calibration to within approximately 0.5 Å was achieved by a mercury lamp and the effective wavelength resolution on each channel was 5 Å. Although intensity calibration was not necessary for making the nonequilibrium temperature measurements, it was felt that a photometric survey would serve to

investigate impurity effects as well as obtain an independent check on the f number for the $N_2^+(1-)$ system.

A monitor channel was also used which employed an S1 surface photomultiplier with a cut-off filter at 5500 Å.

c) Measurements

Shock tube spectra such as those in Fig. 1 show the $N_2^+(1-)$ radiation to be the prominent radiator from the nonequilibrium and equilibrium regions of incident nitrogen shock between 3500 and 4500 Å, and at temperatures in the vicinity of 7000°K. The $N_2^+(1-)\ \Delta v = +1$ sequence in the vicinity of 4200 Å was used for inferring the rotational and vibrational temperature because the spectra showed this region to be clear of impurity radiation from CN, a commonly found impurity in the $N_2^+(1-)\ \Delta v = 0$ sequence.[8]

The three channels of the monochromator were so spaced that the red and middle channel could be used to measure the rotational temperature of the (0, 1) $N_2^+(1-)$ transition, while the red and blue channel could be used to measure the vibrational temperature by observing the (0, 1) and (2, 3) vibrational $N_2^+(1-)$ transitions. The monitor channel was used to view essentially only the $N_2(1+)$ band system and was identical to that used by Allen et al[1] to observe the $N_2(1+)$ radiation in measuring N_2 recombination rates. Typical oscillograms of photomultiplier signals for these three channels and the monitor channel are shown in Fig. 2. The radiation emitted is from an incident nitrogen shock, $U_s = 6.9$ mm/μsec, $P_1 = 1.0$ mm Hg. The wavelength resolution of each channel was 5 Å. The red channel was centered at 4266 Å, the middle at 4243 Å, and the blue at

4195 Å. These wavelength locations, depicted in Fig. 3, were the positions used for measuring temperature. After going through a maximum, the radiation was observed to decay to an equilibrium level. The equilibrium region as shown in Fig. 1 was found to extend for approximately 20 μsec. Figure 3 shows a wavelength survey obtained with various monochromator settings for repeated shock tube runs at 6.9 mm/μsec. The theoretical curves in the figure are discussed in the next section.

III. EQUILIBRIUM RADIATION

a) Equilibrium Radiation Distribution

The $N_2^+(1-)$ system lends itself well to making rotational or vibrational temperature measurements. The spectroscopic constants for this system are well known,[9] and its band structure is relatively easy to calculate. Since it is a $^2\Sigma$-$^2\Sigma$ transition, there is no Q branch. From the Fortrat parabola given by

$$\tilde{\nu} = 23391.22 + 3.976\ m + .172\ m^2 \qquad (1)$$

the wavelength location of each rotational line of the (0, 1) vibrational transition was located and plotted as shown in Fig. 4 by the dots. $\tilde{\nu}$ is in cm^{-1}; $m = J'$ for P and $m = J' + 1$ for R branch transitions. J' is the rotational quantum number and the $'$ refers to the emitting states. The intensity of each line for 6500°K is also indicated and is proportional to

$$I \sim \frac{S_J}{T_r}\ e^{-F(J')\frac{hc}{kT_r}} \qquad (2)$$

$S_J = J'$ for R branch and $S_J = J' + 1$ for P branch $^2\Sigma$-$^2\Sigma$ transitions. T_r

is the rotational temperature; h, c and k are the are the usual constants; and F (J') is the rotational term value.

Our experimental resolution, 5 Å, was incapable of resolving the fine structure; hence, although each individual line of the P and R branches was composed of three components, for the purposes of this analysis it was assumed that they were not split. Since the 5 Å experimental resolution was also wider than twice the rotational line spacing, no alternation of intensity between successive rotational transitions was assumed. This alternation is associated with the nuclear spin of homonuclear molecules. The resolution function characteristic of each channel of the monochromator is shown and was folded with the spectrum. The result is shown in the lower part of the figure together with an approximation which assumes $\Delta J = 0$ and then shifts the band edge from the band origin to the band head.

Although this approximation which assumes $\Delta J = 0$ gives insufficient detail of the wavelength structure to allow accurate rotational temperature measurements, it does give enough detail for vibration temperatures. This approximation is used separately by Keck et al[8, 10] and Patch[11] in developing the expression for the radiation intensity from an optically thin gas sample at thermodynamic equilibrium. This expression[10] is, after replacing the constants by their proper values:

$$\frac{dI}{dV\,d\Omega\,d\lambda} = 3.19 \times 10^{-34} \left| \frac{R_{(\bar{r})}}{ea_o} \right|^2 N \phi \tilde{\nu}^6 \quad \frac{hc}{kT_r} \quad e^{-\frac{hc\tilde{\nu}_{oo}}{kT_e}} \frac{w}{cm^3\text{-}\mu\text{-ster}} \tag{3}$$

The symbols are as those given in Ref. 10 where $R_{(\bar{r})}$ is the dipole matrix element for the transition and may be a function of the internuclear separation. a_o is the radius of the first Bohr orbit and e is the charge of the electron. N is the number of molecules in the absorbing state which is not necessarily the ground state, and h, c, and k are the usual constants. T_r, T_v and T_e are the rotational, vibrational and electronic temperatures, respectively. The oscillator strength is related to the matrix element by the expression,

$$f_{v'v''} = \left(\frac{\tilde{\nu}}{3\,R_\infty}\right)\left|\frac{R_{(\bar{r})}}{e\,a_o}\right|^2 \tag{4}$$

where R_∞ is the Rydberg.

$$\phi = \frac{kT_r}{hc}\quad\frac{1}{Q_v''\,Q_r''\,(B_e' - B_e'')}\sum_{\epsilon_r' \geq 0} q_{v'v''}\, e^{-\left(\frac{\epsilon_v' k}{T_v} + \frac{\epsilon_r' k}{T_r}\right)} \tag{5}$$

where: $Q_v'' = \left[1 - \exp\left(-hc\omega_e''/kT_v\right)\right]^{-1}$ is the vibrational partition function for the absorbing state, (the ' refers to the excited electronic or emitting state, and the " refers to lower electronic or absorbing state);

$Q_r'' = kT_r/hcB_e''$ is the rotational partition function for the absorbing state;

$q_{v'v''}$ is the Condon factor for the transition from v' to v";

$\tilde{\nu}_v = \omega_e\,(v + 1/2) - \omega_e\,x_e\,(v + 1/2)^2 + \omega_e\,y_e\,(v + 1/2)^3$ is the wave number of the v^{th} vibrational level;

$\tilde{\nu}_{v'v''} = \nu_{oo} + (\tilde{\nu}_{v'} - \tilde{\nu}_{o'}) - (\tilde{\nu}_{v''} - \tilde{\nu}_{o''})$ is the wave number for the vibrational transition between states v' and v";

$\epsilon_{v'} = hc\,(\tilde{\nu}_{v'} - \tilde{\nu}_{o'})$ is the vibrational energy relative to the ground vibrational state for the emitting state;

$\epsilon_{r'} = B_{e'}/(B_{e'} - B_{e''})\ hc\ (\tilde{\nu} - \tilde{\nu}_{v'v''})$ is the rotational energy for the emitting state, with the approximation made that the rotational quantum number J does not change in a given transition.

In a transition, J can change by + 1, 0 or - 1 giving R, Q and P branches, respectively. However, for increasing rotational temperatures where high J values are more heavily weighted or where the spectrum is observed with coarse resolution, the effect of $\Delta J \pm 1$ is washed out. The degree to which this approximation matches the detailed calculation for the rotational structure is shown in Fig. 4. Although it lacks detail within an interval $\Delta\tilde{\nu} \sim B_e^2/\Delta B_e$ of the band head, $\phi\ \tilde{\nu}^6$ gives a good description of the vibrational structure.

ϕ and related parameters were calculated for the $N_2^+(1-)$ system over the whole spectrum. The Franck-Condon factors of Nicholls[12] were used for the calculation. Extracts from the computer program are shown in Table I over the temperature and wavelength region of interest to this experiment. A diagram of the relationship between the tabulated parameters and the spectra is shown in Fig. 5. ϕ_1 represents the sum of all contributions from vibrational transitions occurring at longer wavelengths. This program also accounted for the interaction of vibration on the rotational structure. This effect is displayed in the α column where α at a given temperature varies slightly from one vibrational transition to another.

$$\alpha = \frac{B_e'}{(B_e' - B_e'')}\ \frac{hc}{kT_r} \qquad (6)$$

The value of ϕ at the band origin for a given vibrational transition is given by:

$$\Delta\phi = \frac{B''_e}{Q''_v (B'_e - B''_e)} q_{v'v''} e^{-\frac{hc(\tilde{\nu}_{v'} - \tilde{\nu}_{o'})}{kT_v}} \quad (7)$$

$\Delta\phi$ is a function of the vibrational temperature T_v, while α is a function of the rotational temperature T_r.

b) $N_2^+(1-)$ f Number Measurement

By combining the $\Delta J = 0$ approximation with the detailed rotational structure calculation, a theory line was constructed through the data displayed in Fig. 3. The theory line was normalized to the data by a $\left|\frac{R(\bar{r})}{a_o e}\right|^2$ value of .45 $\pm$ .06 and assuming no internuclear separation dependence. This value corresponds to an f number defined at 3914 Å, the 0, 0 transition of .035, with a standard deviation of $\pm$ .005. This value is in accord with the value of .0348 measured by Bennet and Dalby[13] using a radiative lifetime technique. It is also in agreement with the value of .032 measured by Shumaker[14] from a nitrogen arc. Also plotted in the figure is the possible contribution that the $N_2(2+)$ system might make based on the f number of 0.09 reported in Ref. 8. Contributions from this source are neglected in the temperature analysis, since probably only second-order effects would be produced.

The $N_2^+(1-)$ f number of .035 used in conjunction with the ϕ program together with up-to-date Franck-Condon factors generate radiation intensity levels which match well the measurements of Allen et al[7] displayed in Fig. 6. The spectral distribution of the $N_2(1+)$ system was also programmed[12] and a theory line was calculated using an f number at the $N_2(1+)$, (0, 0) transition of .005 and no internuclear separation dependence. The situation regarding

the f number for this system is still unsettled due to various interpretations by different workers of the radiation emitted from air and nitrogen shocks,[10] and the $N_2(1+)$ theory line in the figure is intended primarily for comparison.

IV. NONEQUILIBRIUM TEMPERATURES

a) Rotational Temperature

The rotational temperature T_r was inferred from a change in spectral distribution relative to an equilibrium distribution. The red and middle channels depicted in Fig. 3 were used as a two-channel uncalibrated system to measure the rotational temperature. The advantage of using an uncalibrated system was that a change in spectral distribution was more easily detected by normalizing the outputs of the two channels to their corresponding equilibrium values. This was equivalent to using the equilibrium radiation as the calibration source. For a given equilibrium temperature, the resultant expression for this normalized ratio as a function G_r of T_r and T_e was:

$$\left(\frac{I}{I\,eq.}\right)_M \left(\frac{I\,eq.}{I}\right)_R = G_r\,(T_r, T_e) \tag{8}$$

where M refers to the middle channel which has higher J' values than the red channel. Figure 7(a) shows calculations for G_r versus T_r for an equilibrium temperature of 7000°K, and for the monochromator settings depicted in Fig. 3. Both the detailed and $\Delta J = 0$ calculation assumed a smeared rotational line model. As pointed out before, the use of this model was justified since the experimental resolution was more than twice the rotational line spacing in either the P or R branches. The detailed calculation separated the P and R branches. It was obtained by using a smeared line model applied to the two branches separately, and then summing the two contributions at the

central wavelength of each channel. The $\Delta J = 0$ approximation was calculated by applying the smeared line model to a Q branch only. Several incident nitrogen shocks were analyzed. The results of a typical run are shown in Fig. 8. The open circles indicate the measured rotational temperature. Since the radiation observed by both the red and middle channels was that of the (0, 1) $N_2^+(1-)$ transition, it was assumed that G_r was not a function of T_v.

b) Vibrational Temperature

The spectral distribution to be expected from a radiating gas which has a vibrational temperature different than its rotational temperature can easily be calculated by extracting from calculations such as those shown in Table I, the $\Delta\phi$'s for one temperature, and the α's for another. $\Delta\phi$ and α have been previously defined and are the parameters which determine the vibrational and rotational structure of the radiation, respectively.

The uncalibrated two-channel system composed of the red and blue channels depicted in Fig. 3 was used to infer nonequilibrium vibrational temperatures by a method similar to that used for obtaining T_r. The expression that resulted was:

$$\left(\frac{I}{I_{eq.}}\right)_B \left(\frac{I_{eq.}}{I}\right)_R = G_v\,(T_v,\ T_r,\ T_{eq.}) \qquad (9)$$

The B refers to the blue channel which in this experiment saw a higher vibrational transition than the red channel, R. G_v was calculated and plotted in Fig. 7(b) versus T_v with T_r and $T_{eq.}$ as parameters.

The vibrational temperature history of the incident shock of Fig. 8 was obtained by first measuring the rotational temperature and applying the results to calculations similar to those shown in Fig. 7(b).

c) Electronic Temperature

The absolute magnitude of the molecular radiation from a high temperature gas is related to an electronic temperature, T_e, and the number in the ground state, by

$$I \sim \frac{N_2}{Q_e} \; e^{-\epsilon_{e'}/kT_e} \tag{10}$$

where N_2 is the concentration of molecules, Q_e is the electronic partition function, and $\epsilon_{e'}$ is the energy of the emitting state relative to the ground state. $\epsilon_{e'}$ can be seen from Eq. (3) to be equal to $\epsilon_{e''} + \frac{hc\,\tilde{\nu}_{00}}{kT_e}$ where $\epsilon_{e''}$ is the energy of the absorbing state above the ground state. For an incident shock, if the concentration history is known, an electronic temperature history can easily be inferred from the radiation history of a molecular radiator. If an equilibrium temperature is assumed, the absolute magnitude of the radiation or the f number for the system need not be known, since the observed nonequilibrium intensity I, is related to the equilibrium intensity by:

$$\frac{I}{I_{eq.}} = \frac{N_2 \; e^{-\epsilon_{e'}/kT_e}}{N_{2\,eq.} \; e^{-\epsilon_{e'}/kT_{eq.}}} \tag{11}$$

The N_2 concentration history of the incident shock of Fig. 8 was assumed to be a constant. An activation energy corresponding to the $N_2(1+)$ system of 85,000°K and the data similar to that shown in Fig. 2(c) was used in conjunction with expression (11) to generate the electronic temperature history shown

in Fig. 8.

These measured temperature histories qualitatively are those expected for an incident shock wave. The rotational temperature is expected to equilibrate in a few mean free paths at the shock front and then follow the translational temperature. The vibrational and electronic temperatures are expected to relax more slowly. There has been some indication that electronic and vibrational degrees of freedom are strongly coupled[3, 8] however, the results of the present study indicate the electronic temperature more strongly coupled to the translational temperature.

Methods developed in the present study should prove very useful for measuring nonequilibrium temperatures in the general study of relaxation processes. The work can be expanded to include measurements from mixtures of gases over a range of conditions. Various constituent radiators and vibrational transitions could also be used in order to verify the assumption of a Boltzmann-like distribution over each mode of carrying energy.

ACKNOWLEDGMENT

The author would like to express appreciation for the helpful suggestions given by J.C. Keck, and also for the assistance of J. Carlson and J. McEachern in the experimental part of the work.

REFERENCES

1. Allen, R.A., Keck, J.C. and Camm, J.C., "Non-Equilibrium Radiation from Shock Heated Nitrogen and a Determination of the Recombination Rate," Avco-Everett Research Laboratory Research Report 110, June 1961.

2. Parkinson, W.H. and Nicholls, R.W., "Spectroscopic Temperature Measurements in a Shock Tube Using CN as a Thermometric Molecule," Can. J. Phys. 38, 715 (1960).

3. Faizullov, F.S., Sobolev, N.N. and Kudryavtsev, E.M., "Spectroscopic Investigation of the State of the Gas Behind a Shock Wave, III," Optics and Spectroscopy 8, 400-404 (1960).

4. Wurster, W.H. and Treanor, C.E., "Spectroscopic Technique for Temperature-Density Measurements in Oxygen-Bearing Flows," Cornell Aeronautical Laboratory Report No. AD-1118-A-10, December 1959.

5. Watson, R., "Experimental Spectroscopic Temperature Measurements in the Reflected Wave Region of a Shock Tube Using the OH $^2\Sigma \rightarrow ^2\pi$ Band System," J. Quant. Spect. Rad. Transf. 3, 255 (1963).

6. Camm, J.C. and Rose, P.H., "Electric Shock Tube for High Velocity Simulation," Avco-Everett Research Laboratory Research Report 136, July 1962.

7. Allen, R.A., Camm, J.C. and Keck, J.C., "Radiation from Hot Nitrogen," J. Quant. Spect. Rad. Transf. 1, 269-277 (1961); also Avco-Everett Research Laboratory Research Report 102, April 1961.

8. Keck, J.C., Camm, J.C., Kivel, B. and Wentink, T. Jr., "Radiation from Hot Air. Part II," Annals of Physics 7, 1-38 (1959); also Avco-Everett Research Laboratory Research Report 42, February 1959.

9. Herzberg, G., Molecular Spectra and Molecular Structure. Vol. I. Spectra of Diatomic Molecules (Van Nostrand Co., Inc. New York, 1950).

10. Keck, J.C., Allen, R.A. and Taylor, R.L., "Electronic Transition Moments for Air Molecules," J. Quant. Spect. Rad. Transf. 3, November 1963; also Avco-Everett Research Laboratory Research Report 149, March 1963.

11. Patch, R.W., Shackleford, W.L. and Penner, S.S., "Approximate Spectral Absorption Coefficient Calculations for Electronic Band Systems Belonging to Diatomic Molecules," J. Quant. Spect. Rad. Transf. 2, 263-271 (1962).

12. Nicholls, R.W., "Transition Probabilities of Molecular Band Systems XVIII: Franck-Condon Factors to High Vibrational Quantum Numbers I: N_2 and N_2^+," The University of Western Ontario Scientific Report No. 6, May 15, 1961.

13. Bennet, R.G. and Dalby, F.W., "Experimental Determination of the Oscillator Strength of the First Negative Bands of N_2^+," J. Chem. Phys. 31, 435 (1959).

14. Zwicker, H. and Schumacher, U., "Spectroscopic Studies of the Energy-Density in Confined Plasmas," Proceedings of the 6th Conference on Ionization Phenomena in Gases, Paris, France, July 8-13, 1963, p.170.

TABLE I

SPECTRAL DISTRIBUTION FUNCTION AND RELATED PARAMETERS N_2^+ (1-) BAND SYSTEM

V'	V"	$\tilde{\nu}$, cm^{-1}	λ, Å	ϕ_2	$\Delta\phi$	$\phi_1 \tilde{\nu}^6$, cm^{-6}	$\phi_2 \tilde{\nu}^6$, cm^{-6}	α	$\int \phi \tilde{\nu}^6 d\lambda$ cm^{-5}
					4,000°K				
19	19	23237.0	4303.5	3.1653E-03	3.6705E-07	4.7025E 23	4.7831E 23	3.8101E-03	7.2239E 19
29	21	23268.6	4297.6	2.5136E-03	2.0839E-06	4.4656E 23	4.4656E 23	9.4320E-02	7.2326E 19
21	20	23305.0	4290.9	2.4659E-03	9.0462E-06	3.9362E 23	3.9507E 23	4.2219E-03	7.2354E 19
24	21	23325.1	4287.2	2.2904E-03	2.4072E-06	3.6746E 23	3.6885E 23	5.5923E-03	7.2369E 19
0	1	23391.2	4275.1	1.5616E 00	1.5600E 00	2.5026E 23	2.5578E 26	4.3547E-03	7.2406E 19
28	21	23550.0	4246.3	7.8208E-01	2.7827E-08	1.3341E 26	1.3341E 26	2.1757E-02	1.2665E 20
15	16	23550.1	4246.3	7.8177E-01	3.6366E-06	1.3336E 26	1.3336E 26	3.5834E-03	1.2667E 20
25	21	23577.4	4241.3	6.9406E-01	4.0877E-09	1.1923E 26	1.1923E 26	6.8107E-03	1.3288E 20
1	2	23620.8	4233.6	1.2992E 00	7.2458E-01	9.9804E 25	2.2565E 26	4.3012E-03	1.4138E 20
27	21	23693.2	4220.6	9.4999E-01	2.1570E-06	1.6806E 26	1.6806E 26	1.2433E-02	1.6666E 20
26	21	23701.2	4219.2	9.1742E-01	3.2383E-07	1.6263E 26	1.6263E 26	8.7686E-03	1.6904E 20
18	18	23831.3	4196.2	5.2270E-01	9.9178E-07	9.5751E 25	9.5751E 25	3.8658E-03	1.9813E 20
2	3	23832.0	4196.0	7.6962E-01	2.4843E-01	9.5490E 25	1.4101E 26	4.2480E-03	1.9824E 20
14	15	23847.0	4193.0	7.1516E-01	5.2495E-06	1.3159E 26	1.3159E 26	3.6328E-03	2.0233E 20
22	20	23923.9	4179.9	5.1840E-01	4.3768E-06	9.7136E 25	9.7136E 25	4.8379E-03	2.1722E 20
3	4	24021.9	4162.9	4.1388E-01	7.3719E-02	6.5361E 25	7.3526E 25	4.1951E-03	2.3091E 20
20	19	24084.1	4152.1	3.1706E-01	1.0607E-05	6.1875E 25	6.1877E 25	4.2865E-03	2.3847E 20
13	14	[illegible]	4151.0	3.0811E-01	7.4029E-06	6.0228E 25	6.0230E 25	3.6825E-03	2.3918E 20
4	5	24187.4	4134.4	2.2334E-01	1.9608E-02	4.0795E 25	4.4721E 25	4.1425E-03	2.4745E 20
					7,000°K				
19	19	23237.0	4303.5	5.5167E-02	4.0531E-05	8.6784E 24	8.6848E 24	[illegible]	1.6765E 20
29	21	23268.6	4297.6	5.1506E-02	3.6607E-06	8.1742E 24	8.1748E 24	5.3897E-02	1.6314E 20
21	20	23305.0	4290.9	4.9943E-02	1.2766E-03	7.6366E 24	7.8411E 24	2.4125E-03	1.6367E 20
24	21	23325.1	4287.2	4.7315E-02	4.2787E-04	7.5308E 24	7.6197E 24	3.1956E-03	1.6396E 20
0	1	23391.2	4275.1	1.0773E 00	1.0363E 00	6.7245E 24	1.7647E 26	2.4884E-03	1.6483E 20
28	21	23550.0	4246.3	7.2720E-01	5.1207E-06	1.2495E 26	1.2405E 26	1.2432E-02	2.0772E 20
15	16	23550.1	4246.3	7.2724E-01	2.0256E-06	1.2403E 26	1.2406E 26	2.0477E-03	2.0774E 20
25	21	23577.4	4241.3	6.7962E-01	7.5540E-07	1.1675E 26	1.1675E 26	3.8918E-03	2.1367E 20
1	2	23620.8	4233.6	1.3043E 00	6.9777E-01	1.0604E 26	2.2654E 26	2.4578E-03	2.2232E 20
27	21	23693.2	4220.6	1.0915E 00	4.0579E-04	1.7303E 26	1.9310E 26	7.1044E-03	2.4940E 20
26	21	23701.2	4219.2	1.0761E 00	6.0796E-05	1.8760E 26	[illegible]	5.0106E-03	2.5715E 20
18	18	23831.3	[illegible]	7.7640E-01	[illegible]	1.4222E 26	1.4224E 26	2.7050E-03	[illegible]
2	3	[illegible]	[illegible]	[illegible]	3.4017E-01	[illegible]	2.0436E 26	2.4274E-03	2.9029E 20
14	15	[illegible]	[illegible]	[illegible]	[illegible]	1.9082E 26	1.9666E 26	2.0757E-03	2.9631E 20
22	20	23923.9	4179.9	8.2107E-01	6.7750E-04	1.6704E 26	1.6707E 26	2.7645E-03	3.2012E 20
3	4	[illegible]	4162.9	8.4378E-01	1.4315E-01	[illegible]	1.6213E 26	2.3972E-03	3.4574E 20
20	19	24084.1	4152.1	[illegible]	1.3366E-03	1.4144E 26	1.4170E 26	2.4494E-03	3.6205E 20
13	14	[illegible]	4151.0	7.1455E-01	2.6715E-06	[illegible]	[illegible]	2.1043E-03	3.6367E 20
4	5	[illegible]	4134.4	[illegible]	[illegible]	[illegible]	1.2370E 26	2.3672E-03	3.8454E 20
					10,000°K				
29	21	[illegible]	[illegible]	[illegible]	[illegible]	2.4346E 25	[illegible]	3.7728E-02	2.5410E 20
21	20	[illegible]	[illegible]	[illegible]	[illegible]	[illegible]	[illegible]	1.6888E-03	2.5568E 20
24	21	[illegible]	[illegible]	[illegible]	2.7831E-03	2.3701E 25	[illegible]	2.2367E-03	2.5656E 20
0	1	[illegible]	[illegible]	9.0832E-01	7.7243E-01	[illegible]	1.4875E 26	1.7413E-03	2.5938E 20
28	21	[illegible]	[illegible]	[illegible]	[illegible]	[illegible]	[illegible]	8.7026E-03	2.9770E 20
15	16	[illegible]	[illegible]	[illegible]	[illegible]	[illegible]	1.1831E 26	1.4334E-03	2.9772E 20
25	21	23577.4	[illegible]	[illegible]	[illegible]	1.1471E 26	1.1371E 26	2.7243E-03	3.0343E 20
1	2	[illegible]	4233.6	1.2134E 00	[illegible]	[illegible]	2.1075E 26	1.7205E-03	3.1200E 20
27	21	[illegible]	4220.6	[illegible]	[illegible]	[illegible]	1.9014E 26	4.9731E-03	3.3787E 20
26	21	[illegible]	[illegible]	[illegible]	[illegible]	[illegible]	[illegible]	3.5074E-03	3.4059E 20
18	18	[illegible]	[illegible]	[illegible]	[illegible]	[illegible]	1.5542E 26	1.5463E-03	3.6001E 20
2	3	[illegible]	[illegible]	1.1661E 00	[illegible]	[illegible]	2.1731E 26	1.6992E-03	3.8019E 20
14	15	[illegible]	[illegible]	[illegible]	[illegible]	[illegible]	2.1214E 26	1.4531E-03	3.8663E 20
22	20	[illegible]	[illegible]	[illegible]	[illegible]	[illegible]	[illegible]	1.7352E-03	4.1297E 20
3	4	[illegible]	[illegible]	[illegible]	[illegible]	[illegible]	[illegible]	1.6780E-03	4.4335E 20
20	19	[illegible]	[illegible]	[illegible]	[illegible]	[illegible]	[illegible]	1.7146E-03	4.6361E 20
13	14	[illegible]	[illegible]	[illegible]	[illegible]	[illegible]	[illegible]	1.4730E-03	4.6970E 20
4	5	[illegible]	[illegible]	[illegible]	[illegible]	[illegible]	1.7043E 26	1.6573E-03	4.9355E 20
					15,000°K				
19	19	[illegible]	4303.5	[illegible]	[illegible]	[illegible]	[illegible]	1.0160E-03	3.7743E 20
29	21	[illegible]	4297.6	3.3770E-01	[illegible]	[illegible]	[illegible]	2.5152E-02	3.8062E 20
21	20	[illegible]	[illegible]	[illegible]	[illegible]	[illegible]	[illegible]	1.1258E-03	3.6419E 20
24	21	23325.1	4287.2	[illegible]	[illegible]	[illegible]	[illegible]	1.4713E-03	3.8679E 20
0	1	[illegible]	4275.1	[illegible]	5.6129E-01	[illegible]	1.4423E 26	1.1613E-03	3.9320E 20
28	21	[illegible]	4246.3	7.3935E-01	1.4594E-04	1.2610E 26	1.2612E 26	5.8017E-03	4.3212E 20
15	16	[illegible]	[illegible]	[illegible]	2.4670E-03	1.2511E 26	1.2654E 26	9.5555E-04	4.3214E 20
25	21	23577.4	4241.3	7.1978E-01	2.1534E-05	1.2364E 26	[illegible]	1.8162E-03	4.3630E 20
1	2	[illegible]	4233.6	1.1563E 00	4.7030E-01	1.1372E 26	2.0083E 26	1.1475E-03	4.4774E 20
27	21	[illegible]	4220.6	1.0791E 00	1.1748E-02	1.8364E 26	1.9071E 26	3.3154E-03	4.7292E 20
26	21	23701.2	[illegible]	1.0670E 00	1.7674E-03	1.8735E 26	1.8966E 26	2.3383E-03	4.7565E 20
18	18	23831.3	4196.2	9.2414E-01	1.6910E-03	1.6693E 26	1.6929E 26	1.0309E-03	5.1691E 20
2	3	[illegible]	4196.0	1.2296E 00	2.7720E-01	1.6419E 26	2.2364E 26	1.1328E-03	5.1711E 20
14	15	[illegible]	4193.0	1.1997E 00	2.4879E-03	2.2029E 26	2.2075E 26	9.6875E-04	5.2377E 20
22	20	[illegible]	4179.9	1.1173E 00	1.7151E-02	2.0665E 26	2.0987E 26	1.2901E-03	5.5179E 20
3	4	24021.9	4162.9	1.1620E 00	1.6033E-01	1.9247E 26	2.2328E 26	1.1187E-03	5.8607E 20
20	19	24084.1	4152.1	1.1122E 00	2.2102E-02	2.1138E 26	2.1706E 26	1.1431E-03	6.0944E 20
13	14	[illegible]	4151.0	1.1063E 00	2.3305E-03	2.1573E 26	2.1625E 26	9.8200E-04	6.1174E 20
4	5	[illegible]	4134.4	[illegible]	7.6361E-02	[illegible]	2.1373E 26	1.1047E-03	5.4633E 20
					20,000°K				
19	19	[illegible]	[illegible]	[illegible]	1.3728E-03	[illegible]	[illegible]	7.6203E-04	4.6641E 20
29	21	[illegible]	4297.6	6.3930E-01	1.3640E-04	7.3312E 25	7.3342E 25	1.8664E-02	4.7108E 20
21	20	[illegible]	4290.9	6.4005E-01	5.3334E-02	7.7078E 25	8.6522E 25	8.4438E-04	4.7636E 20
24	21	[illegible]	4287.2	5.5388E-01	2.1832E-02	8.5082E 25	8.9196E 25	1.1185E-03	4.7954E 20
0	1	[illegible]	4275.1	7.4321E-01	4.1637E-01	8.6299E 25	1.5450E 26	8.7095E-04	4.9018E 20
28	21	[illegible]	4246.3	6.3023E-01	7.6726E-04	1.6156E 26	1.4163E 26	4.3513E-03	5.3283E 20
15	16	[illegible]	4246.3	8.3375E-01	3.7808E-03	1.4162E 26	1.4226E 26	7.1668E-04	5.3286E 20
25	21	23577.4	4241.3	8.1583E-01	3.7866E-05	1.4014E 26	1.4015E 26	1.3621E-03	5.3981E 20
1	2	[illegible]	4233.6	1.1706E 00	3.6268E-01	1.3684E 26	2.0331E 26	8.6024E-04	5.5058E 20
27	21	[illegible]	4220.6	1.1247E 00	2.1749E-02	1.9311E 26	1.9876E 26	2.4866E-03	5.7634E 20
26	21	[illegible]	4219.2	1.1202E 00	3.2727E-03	1.9400E 26	1.8858E 26	1.7537E-03	5.7320E 20
18	18	23831.3	4196.2	1.0054E 00	2.8168E-03	1.8366E 26	1.8418E 26	7.7316E-04	6.2319E 20
2	3	[illegible]	4196.0	1.2607E 00	2.5583E-01	1.8411E 26	2.3098E 26	8.4960E-04	6.2341E 20
14	15	[illegible]	4193.0	1.2463E 00	3.6889E-03	2.2564E 26	2.2932E 26	7.2656E-04	6.3030E 20
22	20	[illegible]	4179.9	1.2006E 00	3.0835E-02	2.1933E 26	2.2511E 26	9.6759E-04	6.5972E 20
3	4	24021.9	4162.9	1.2598E 00	1.4572E-01	2.1234E 26	2.4034E 26	8.3902E-04	6.9701E 20
20	19	24084.1	4152.1	1.2375E 00	5.0621E-02	2.3162E 26	2.4150E 26	8.5730E-04	7.2239E 20
13	14	[illegible]	4151.0	1.2339E 00	3.4231E-03	2.4054E 26	2.4121E 26	7.3650E-04	7.2517E 20
4	5	[illegible]	4134.4	1.2107E 00	7.3178E-02	2.2778E 26	2.4243E 26	8.2850E-04	7.6405E 20

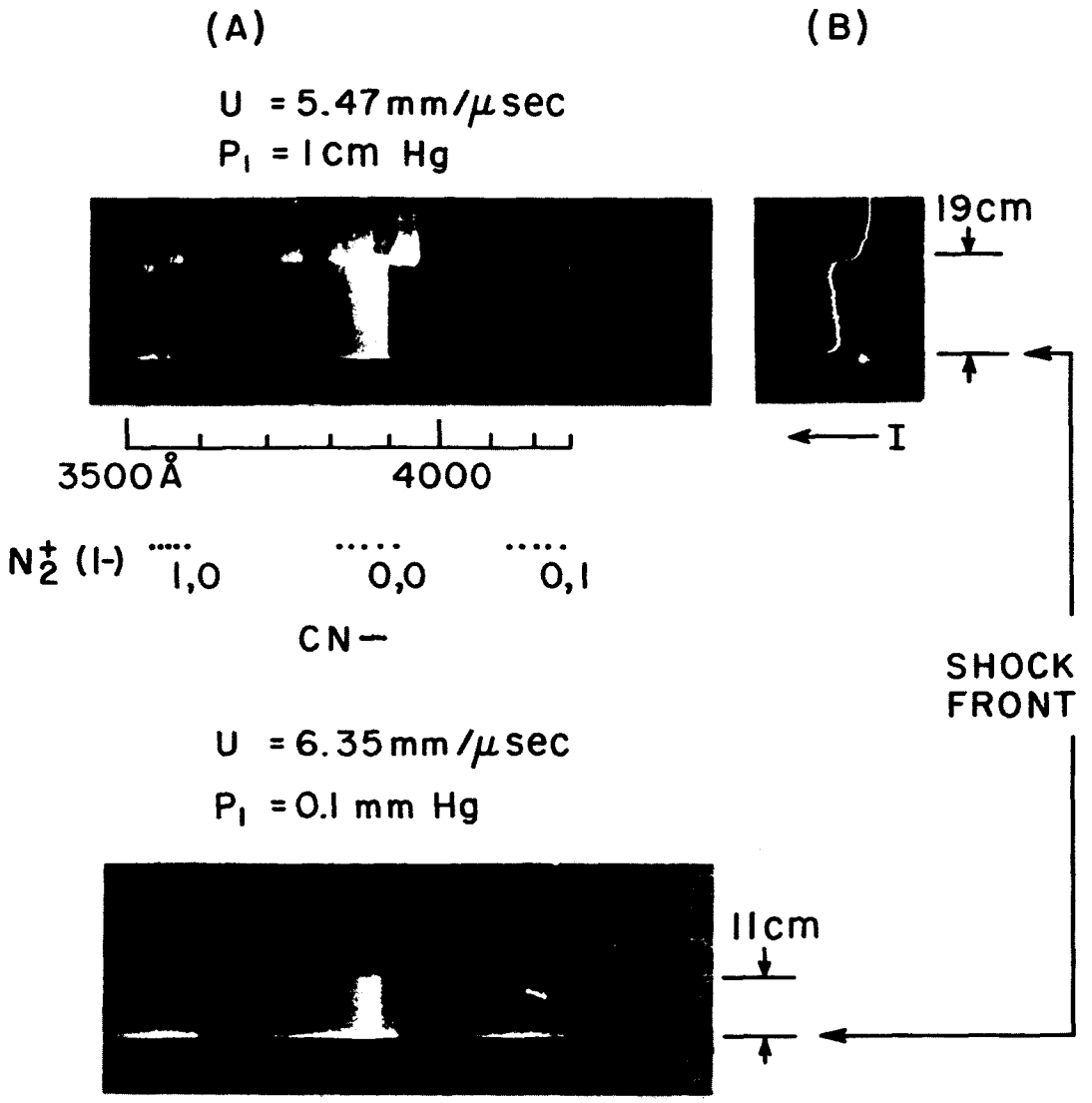

Fig. 1 A. Race track spectrograms of shock waves in nitrogen. The overshoot and equilibrium radiation of the $N_2^+(1-)$ radiation is clearly identified.

B. Oscillogram record of radiation observed in the .55 - 1.1 μ region showing the radiative overshoot and relatively flat equilibrium region. All pictures on the top line are scaled to the same shock thickness.

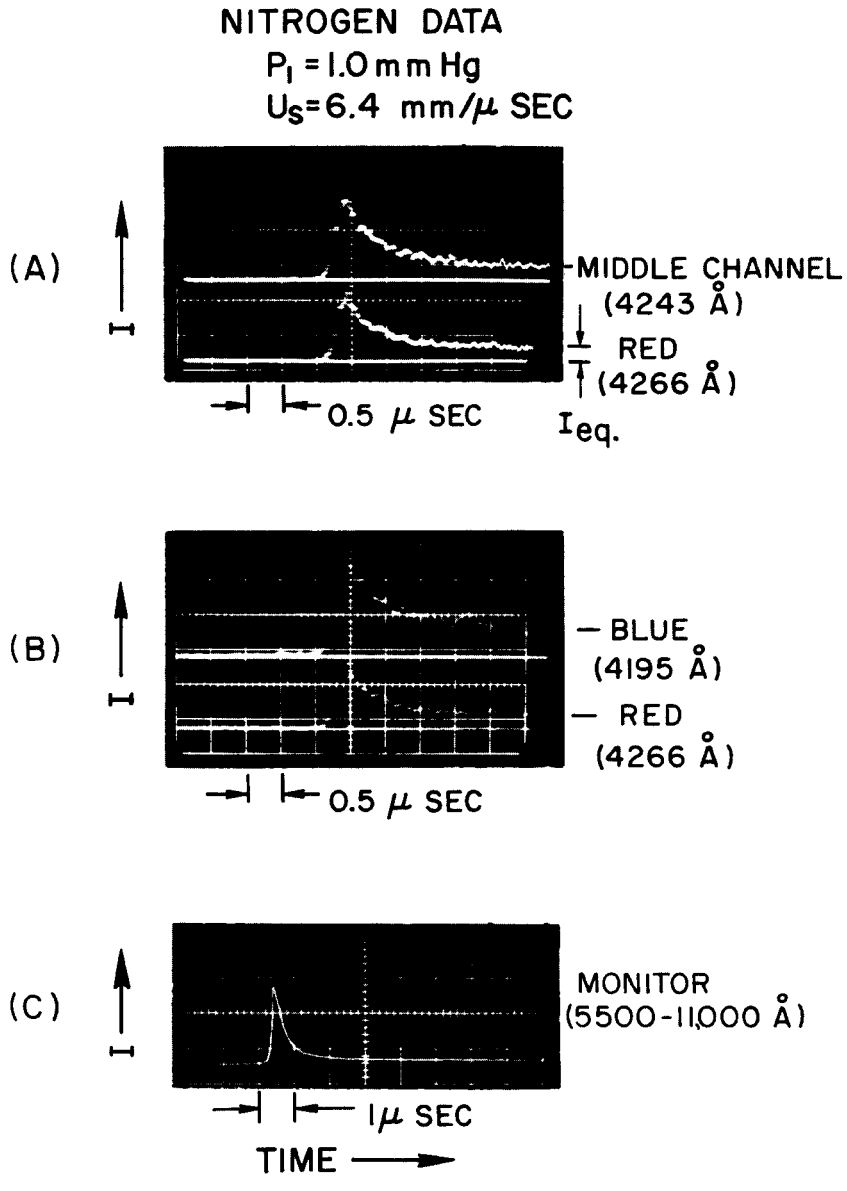

Fig. 2 Oscillogram records of the radiation from an incident shock in nitrogen. The red, middle and blue channels of (A) and (B) have a wavelength resolution of 5 Å and are located to view the various vibration rotational lines of the $N_2^+(1-)$ system in such a way that the vibrational and rotational temperature histories can be inferred. (C) views the $N_2^+(1+)$ radiation from which the electronic temperature history can be inferred.

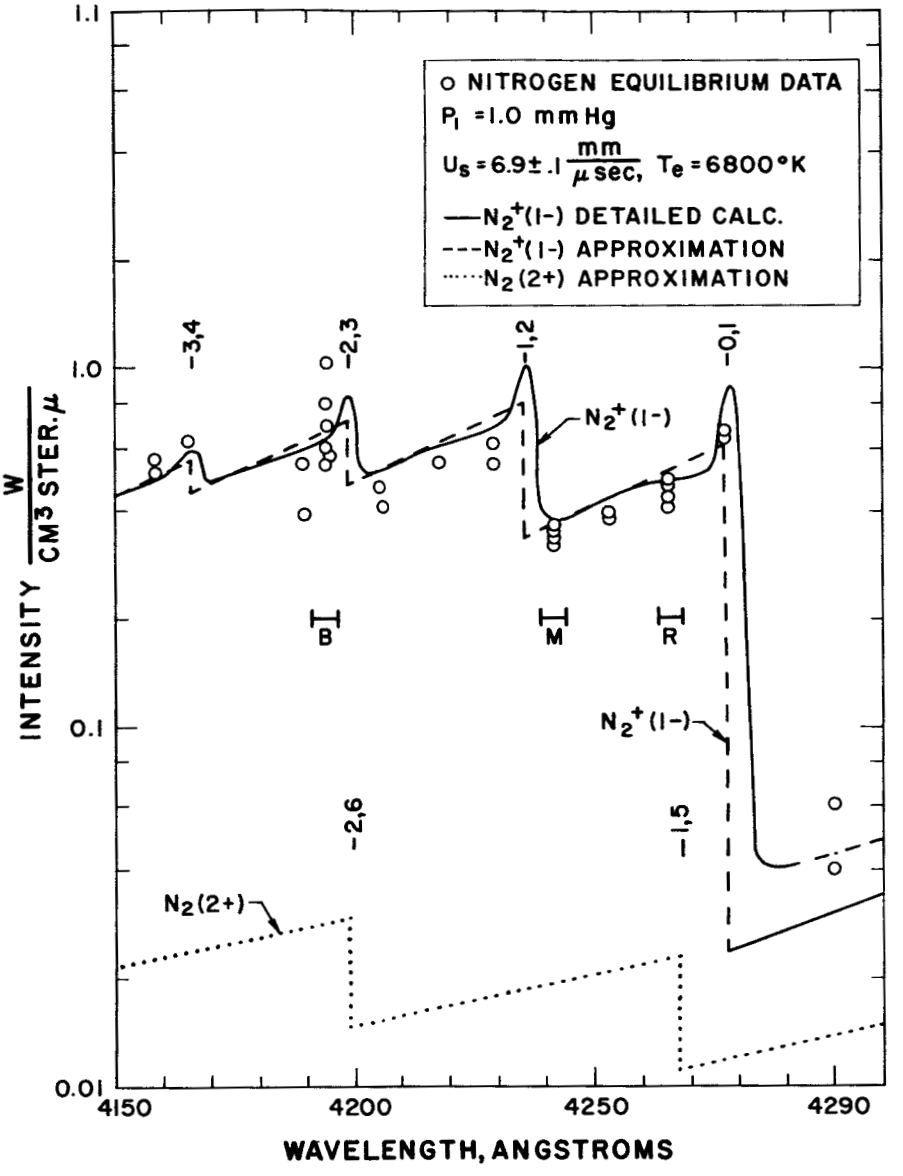

Fig. 3 Equilibrium nitrogen data obtained with a triple channel monochromator with 5 Å resolution in each channel. The 0, 1 $N_2^+(1-)$ band head is clearly located. The solid line is the theoretical calculation for the N_2^+ (1-) system using the method depicted in Fig. 4, and an f number of .035 at the 0, 0 transition with no internuclear separation dependence.

A1635

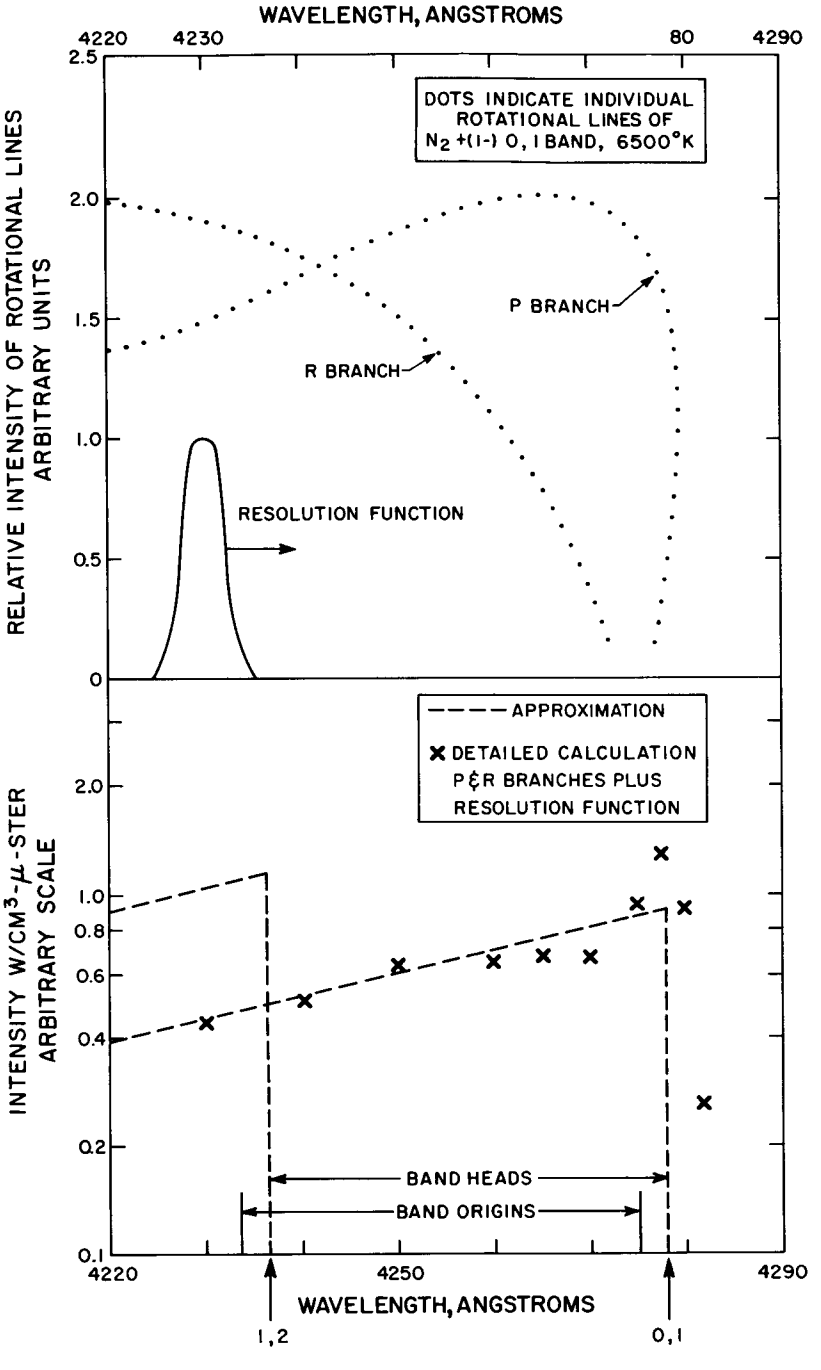

Fig. 4 (Upper) Relative intensity of the individual rotational lines of the P and R branches of the $N_2^+(1-)$ 0, 1 transition versus wavelength at 6500°K. (Lower) Average intensity per unit wavelength as seen by the given resolution function compared with the approximation which assumes $\Delta J = 0$.

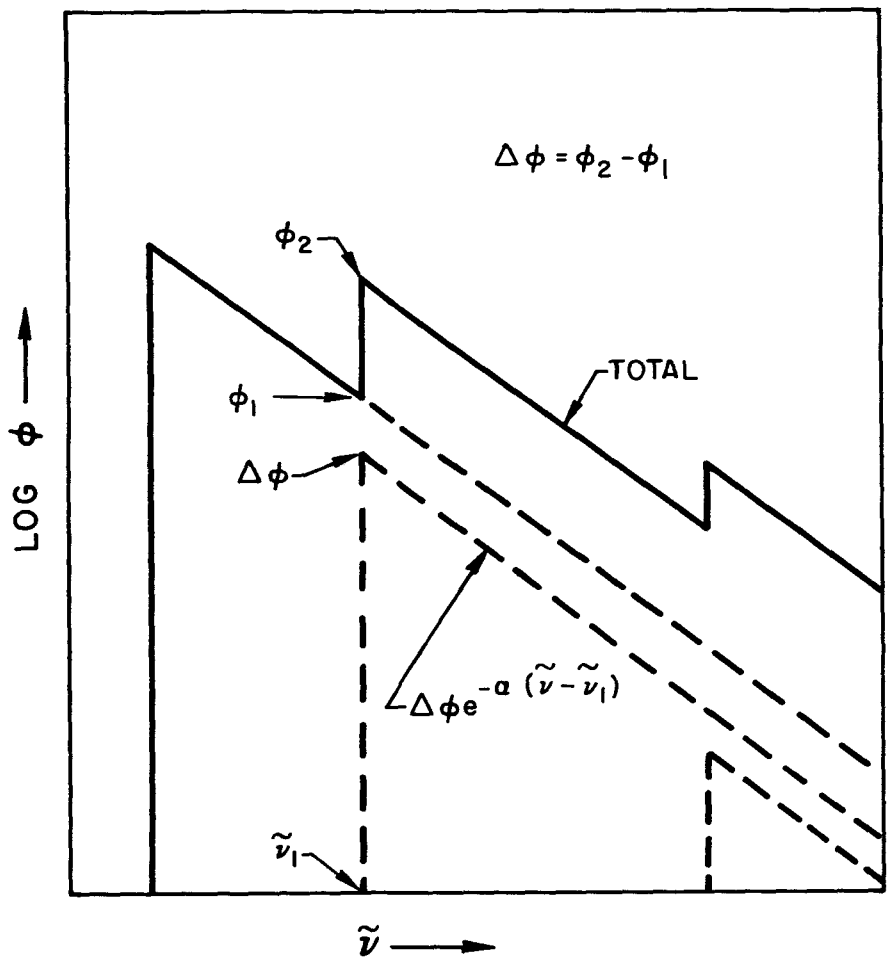

Fig. 5 Diagram showing the relationship between the information of Table I and molecular radiation band structure. The calculation uses a smeared line model and also the approximation which assumes that $\Delta J = 0$, for all vibrational rotational transitions.

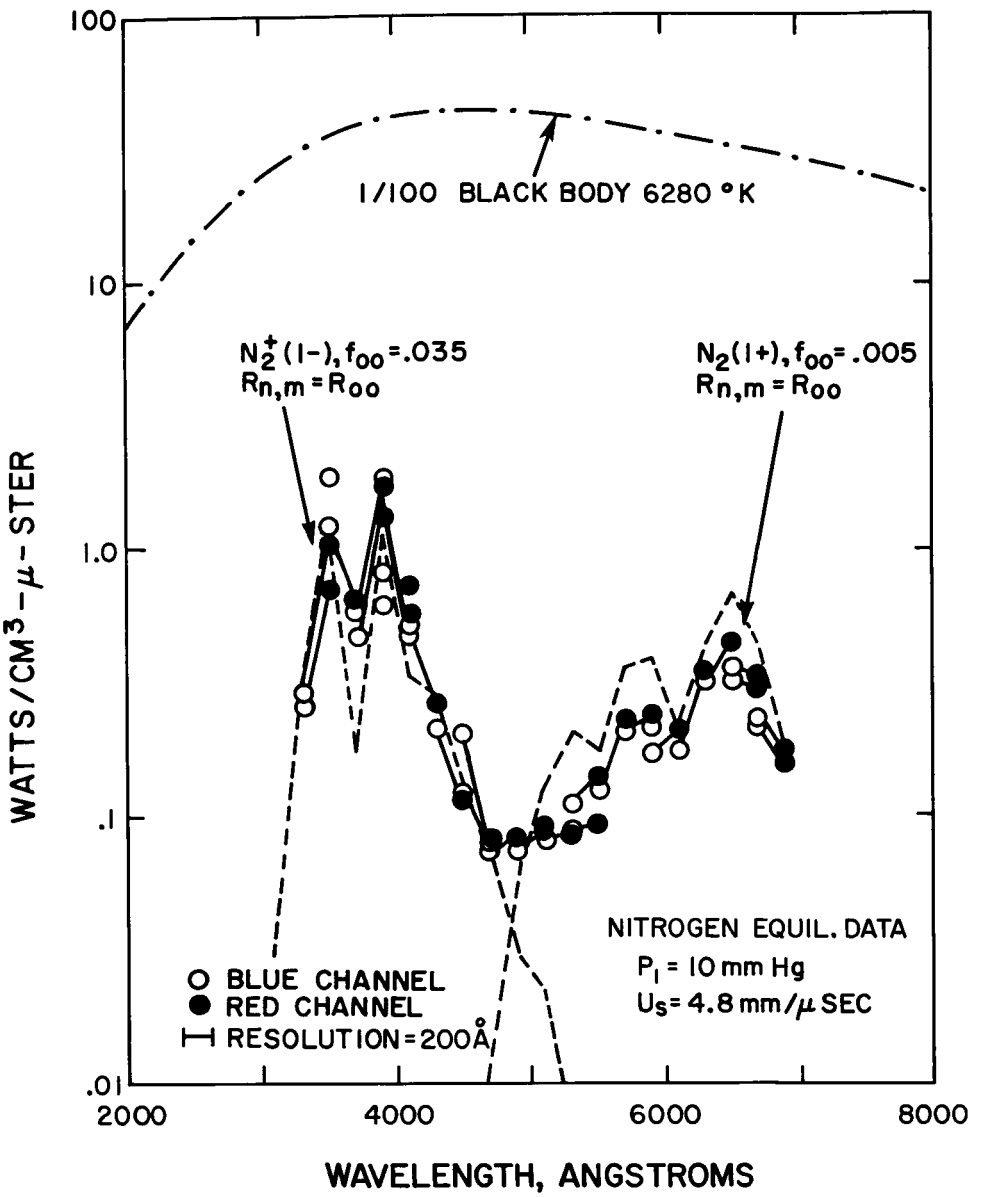

Fig. 6 Equilibrium intensity measurements from Allen et al[14] showing how the presently determined f value of .035 at the 0, 0 transition for the $N_2^+(1-)$ system fits this older data and assuming no internuclear separation dependence for the matrix element. The N_2 (1+) theory line is based on an f number measured at the 0, 0 transition by the author, and also assuming no internuclear separation for the f number.

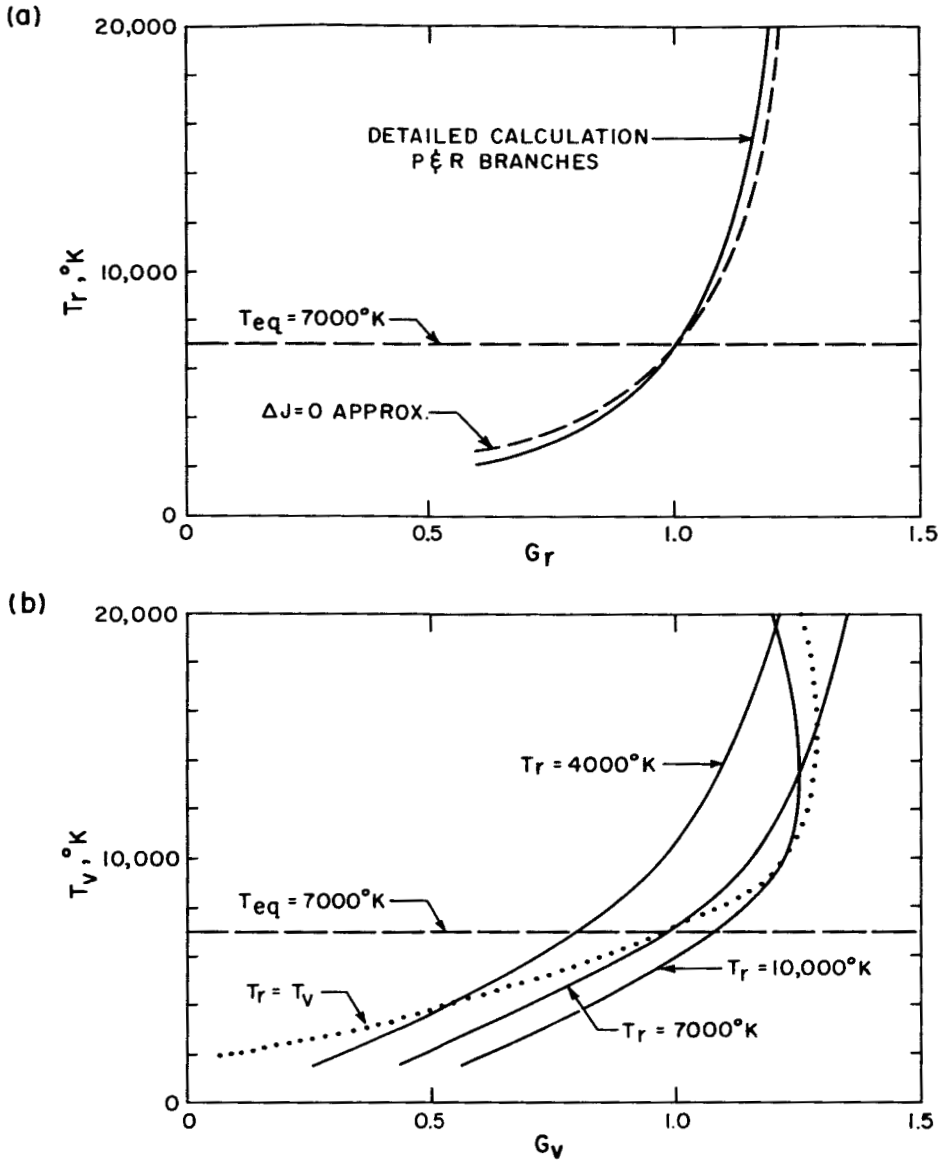

Fig. 7 Curves by which the nonequilibrium rotational (A) and vibrational (B) temperatures can be deduced from measurements for the monochromator settings depicted in Fig. 3 and for an equilibrium temperature of 7000°K. G_r is the ratio of the middle to the red channel intensity normalized to its equilibrium value. G_v is the ratio of the blue to the red channel intensity normalized in the same fashion. T_v inferred from a measured G_v is a function of the rotational temperature, and several curves are plotted for different rotational temperatures.

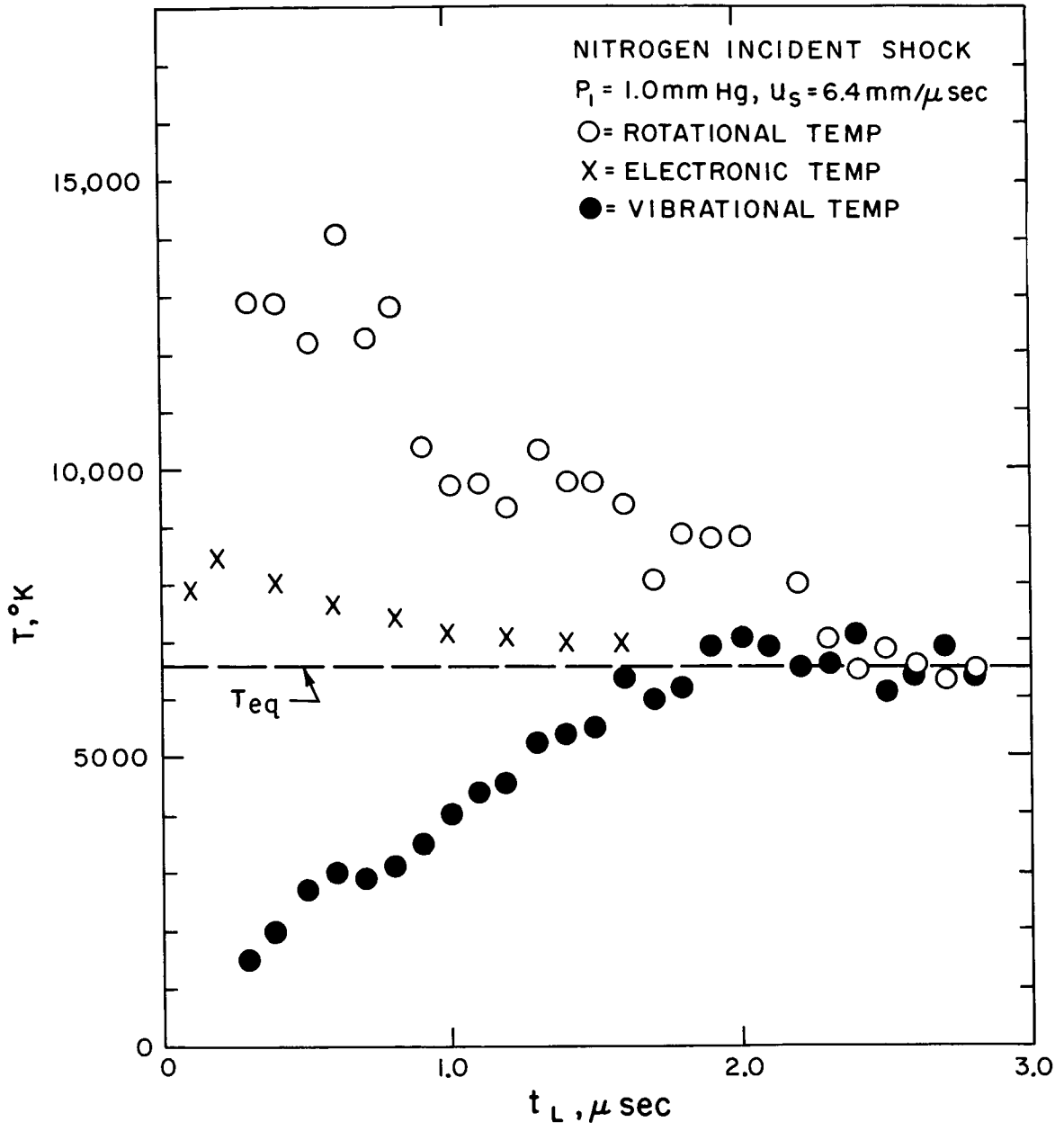

Fig. 8 Measured rotational, vibrational and electronic temperature histories for an incident nitrogen shock. The rotational and vibrational temperatures are those of the excited $N_2^+(B)$ molecule and the electronic temperature is based on the relative populations of the $N_2(X)$ and $N_2(B)$ states.